Focusing Properties of Spirally Polarized Annular Multi Gaussian Beam by High NA Lens

M.Senthilkumar[1], K. B. Rajesh[2]*, M. Udhayakumar[2], K.Prabakaran[3], M. Lavanya[4]
[1]Department of Physics, Research and Development Centre, Bharathiar University, Coimbatore, Tamilnadu, India
[2]Department of Physics, Chikkanna Government Arts College, Tirupur, Tamilnadu, India
[3]Department of Physics, Mahendra Arts and Science College, Namakkal, Tamilnadu, India
[4]Department of Physics, PSGR Krishnammal College for Women, Coimbatore, Tamilnadu, India

ABSTRACT: Focusing properties of spirally polarized annular multi Gaussian beam by High NA Lens are investigated theoretically by vector diffraction theory. Results show that the optical intensity in focal region of spirally polarized annular multi Gaussian beam can be altered considerably by the beam order and spiral parameter. Spiral parameter can induce focal pattern change in axial direction remarkably and many novel focal patterns including optical bubbles, focal hole and focal spots of long focal depth and axially separated focal spots and flattop profile are evolved. We expect such a tunable focal patterns are useful for optical manipulation of micro particles.

KEYWORDS: Focusing property, annular multi Gaussian beam, Vector diffraction theory, High NA Lens.

https://doi.org/10.29294/IJASE.9.1.2022.2607-2616 ©2022 Mahendrapublications.com, All rights reserved

INTRODUCTION

Polarization, as an intrinsic nature of light, plays an important role in engineering the optical field and controlling the interaction of light with matter. In recent years, cylindrical vector (CV) beams have attracted significant interest due to the unique focusing features compared with homogeneously polarized beams [1]. Two extreme cases of CV beams are radially polarized (RP) and azimuthally polarized (AP) beams. It is found that an AP beam can be focused to generate a hollow dark spot with totally transverse polarization for the electric field, whereas it is a strong longitudinally polarized hot spot for the input RP beam [2–4]. The longitudinal component of the focus from such CVB is much stronger than the transversal component, and the size of the longitudinal focus is much smaller than the transversal focus [5]. Focal engineering using radially, azimuthally and cylindrically polarized beams has been studied through engineering the amplitude, phase and polarization. Recently, focusing CVB to a very tight spot was one of the most important topics for optical researches and application including sharper focus [6–10], multiple focal spots [11–14], optical needle [15–18],flat-top focus [19], optical chain [20,21], focal spot array[22–24], optical channel [25–27], optical cage [28–31], and spherical spot [32–35] etc. These new properties led to many potential applications, such as optical trapping and manipulation of particles [36,37], high resolution microscopy [38], optical data storage [39], and electron acceleration [40]. The cylindrical vector beams, most focus has so far been mainly on the tightly focused electric field distributions. However, the presence of phase filters or Amplitude filters makes some applications more difficult or even impossible. Bing Hao and James Leger have recently investigated the numerical aperture (NA) invariant focus shaping using spirally polarized beams. They proposed that spirally polarization is another kind of spatially variant polarization bearing radial symmetry [41]. The spirally polarized beam possesses axially symmetric polarization patterns, with linear polarization at any point of the transverse profile and with the electric field lines being logarithmic spiral. Recent investigation of the tight focusing properties of spirally polarized beam suggested several possible applications such as as optical tweezers, particle trapping, laser cutting, material processing, microscopy, etc.[42–46].The studies of energy flow in the focal plane of optical fields are also important and useful, as they indicate the wide use of such beams in manipulating and transporting absorptive

***Corresponding Author: rajeskb@gmail.com**

Received: 18.06.2022 **Accepted:** 27.07.2022 **Published on**: 01.08.2022

particles [47-48]. In an optical tweezers system, the absorptive particles can be trapped by the strongly focused optical field when absorbing some of the beam energy. Simultaneously, they obtain a fraction of the energy flow, which causes the trapped absorptive particles to move so that the trajectory aligns with the Poynting vector with a velocity that is proportional to the modulus of the Poynting vector. In this paper, we study the energy flow in the focal plane of a tightly focused spirally polarized annular multi Gaussian beam by high NA objective lens based on Richards and Wolf vector diffraction theory, expressions for the electromagnetic fields and the Poynting vector in the focal region are presented. These properties might be helpful in applications such as optical trapping and manipulation of particles and laser processing.

2. THEORY

The state of polarization (SoP) could be mathematically described by the combination of a pair of orthogonal base vectors. When referring to the generalized CV beam, it is given by [47]

$$E_0=\frac{A_0}{\sqrt{2}}\left\{\exp[i(\varphi+\varphi_0)]e_r+\exp[-i(\varphi+\varphi_0)]e_l\right\}=A_0\left[\cos(\varphi+\varphi_0)e_x+\cos(\varphi+\varphi_0)e_y\right]\to(1)$$

where $A_0$is a constant, φ is the azimuthal angle, φ_0 is the initial phase, e_r and e_l represent, respectively, the unit vectors of right-handed and left-handed circular polarization, are unite vectors of linear polarization along x and y axis, respectively .For the incident optical field described in eq.(1), the corresponding three-dimensional electric and magnetic fields near focus can be derived in cylindrical coordinate system (r, φ, z) as [47]

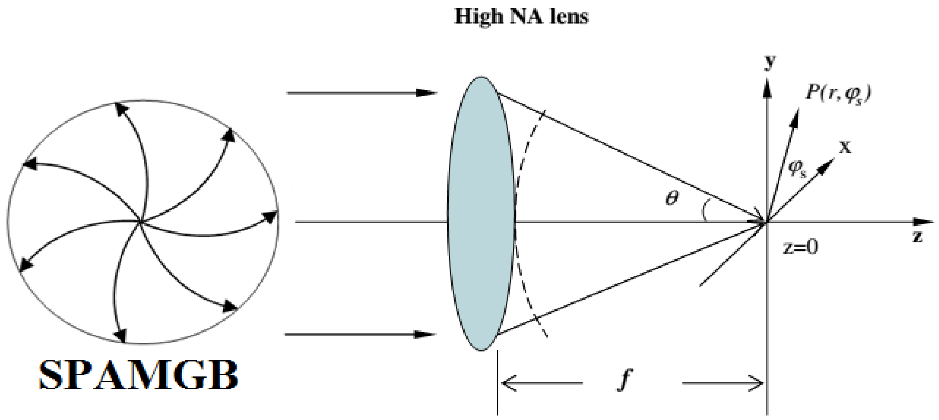

Figure 1 Spirally Polarized Annular Multi Gaussian Beam by high NA focusing system.

$$\begin{bmatrix}E(r,\phi,z)\\H(r,\phi,z)\end{bmatrix}=\frac{-ikf}{2\pi}\int_0^{\alpha}\int_0^{2\pi}\sqrt{\cos\theta}\,l(\theta)\sin\theta\begin{bmatrix}M_E\\M_H\end{bmatrix}\exp(ik_0r)\,d\theta\,d\varphi\to(2)$$

Here, the wave number k = 2π/λ, where λ is the wavelength in free space; f is the focal length of the focusing objective lens; the maximum tangential angle α= arcsin(NA/n), where NA and n are the numerical aperture and the refractive index in the image space that we take as 0.9 and 1, respectively; θ and φ denote, respectively, the tangential angle with respect to z axis and the azimuthal angle with respect to x axis; M_E and M_H represent the propagating electric and magnetic polarization vectors in the image space; k_0 = (-sinθcosφ, -sinθsinφ, cosθ) is the unite vector of the wave vector; r = (rcosφ, rsinφ, z) is the polar vector of arbitrary point in the image space, *l(θ)* is the relative amplitude of the input optical field at the entrance pupil plane.$E_0(\theta)$ Describes the amplitude-modulated annular multi-Gaussian beam, this function is given by [23].

$$l(\theta)=\left(\frac{\theta}{\theta_0}\right)\sum_{n=-N}^{N}\exp\left[-\left(\frac{\theta-\theta_c-n\omega_0}{\omega_0}\right)^2\right]\rightarrow(3)$$

Here, θ is the converging semi-angle. We denote the maximum converging semi-angle as θ_{max} which is related to objective numerical aperture by θ_{max} = arcsin(NA). θ_0 is an angle which, along with integer *m*, determines the shape of the modulation function.θ_0 is usually chosen to be slightly smaller than θ_{max}. θ_c determines the radial position translation of the $l_0(\theta)$ Here we take $\theta_c = \theta_{max}/3$ w_0 is the waist width of single Gaussian beam which is calculated by the following formula

$$\omega_0 := 1/2\times\frac{\alpha}{N+\left\{1-\ln\left[\sum_{n=-N}^{N}\exp(-n^2)\right]\right\}^{1/2}}\rightarrow(4)$$

Equation (3) describes an object beam. The factor (θ/θ_0) measures that the most of light energy is located on the annular edge of the pupil. Increasing the integer *m* will concentrate more energy into the annular edge area in which the converging semi-angle is more than θ_0. The sum of (2N + 1) spatially equally spaced Gaussian beams ensures that the amplitude of the constructed annular multi-Gaussian beam decreases suddenly when reaching the outer edge of the pupil. The Electric and magnetic polarization vectors in terms of M_E *and* M_H can be respectively derived as

$$M_E=\begin{bmatrix}M_E^x\\ M_E^y\\ M_E^z\end{bmatrix}=\begin{bmatrix}-\sin\varphi_0\sin\varphi+\cos\varphi_0\cos\theta\cos\varphi\\ \sin\varphi_0\cos\varphi+\cos\varphi_0\cos\theta\sin\varphi\\ \cos\varphi_0\sin\theta\end{bmatrix}\text{ and}$$

$$M_H=\sqrt{\frac{\varepsilon}{\mu}}\begin{bmatrix}M_H^x\\ M_H^y\\ M_H^z\end{bmatrix}=\begin{bmatrix}-\cos\varphi_0\sin\varphi-\sin\varphi_0\cos\theta\cos\varphi\\ \cos\varphi_0\cos\varphi-\sin\varphi_0\cos\theta\sin\varphi\\ -\sin\varphi_0\sin\theta\end{bmatrix}\rightarrow(5)$$

where, ε and μ denote the dielectric constant and the magnetic permeability of the image space. The term *φ0*in Eq. (1) characterizes the polarization of focusing spirally polarized beam and can be in different forms [12]

$$\varphi_0=\left(C\times\frac{\tan(\theta)}{\tan(\alpha)}\times\pi\right)\rightarrow(6)$$

Where *C* is spiral parameter indicating polarization spiral degree, $\alpha=\arcsin(\mathrm{NA})$ is convergence angle corresponding to the radius of incident optical aperture. In terms of the three-dimensional electric and magnetic field vectors, the energy current can be defined by the time-averaged Poynting vector [25]:

$$P\alpha\frac{c}{8\pi}\mathrm{Re}(\mathrm{E}\times\mathrm{H}^*)\rightarrow(7)$$

where H* the asterisk denotes complex conjugation.

3. RESULTS AND DISCUSSION

Figure 2(a-d) shows 2D intensity distribution of the electric and magnetic field (b,c and e,d) are the corresponding radial and axial intensity distribution of electric and magnetic field.(g-i)shows the transverse , longitudinal and total of the normalized Poynting vector in the through focus plane. In order to study the effect of spiral polarization initially we set the spiral parameter C=0. Figure (a) and (d) shows the intensity distribution of the electric and magnetic field obtained for incident multi Gaussian beam with m=2 and N=20. It is noted from the figure that the generated electric field is a sharper focal spot with dominating the longitudinal component (Ez) whereas the magnetic field is found to have central null with dominating (Mϕ) component. The FWHM and DOF of the electric and magnetic fields are 0.5λ and 1.7λ respectively. The transvers component of the Poynting vector is shown in Figure 2(g) shows that energy flow is inward towards the focus and it is outwards away from the focus with no energy flow along the focus. The longitudinal component also shows null energy flow along the axis and total energy flow is found to be dominated with longitudinal component with no energy flow along the axis are shown in figure 2(h,i)respectively.

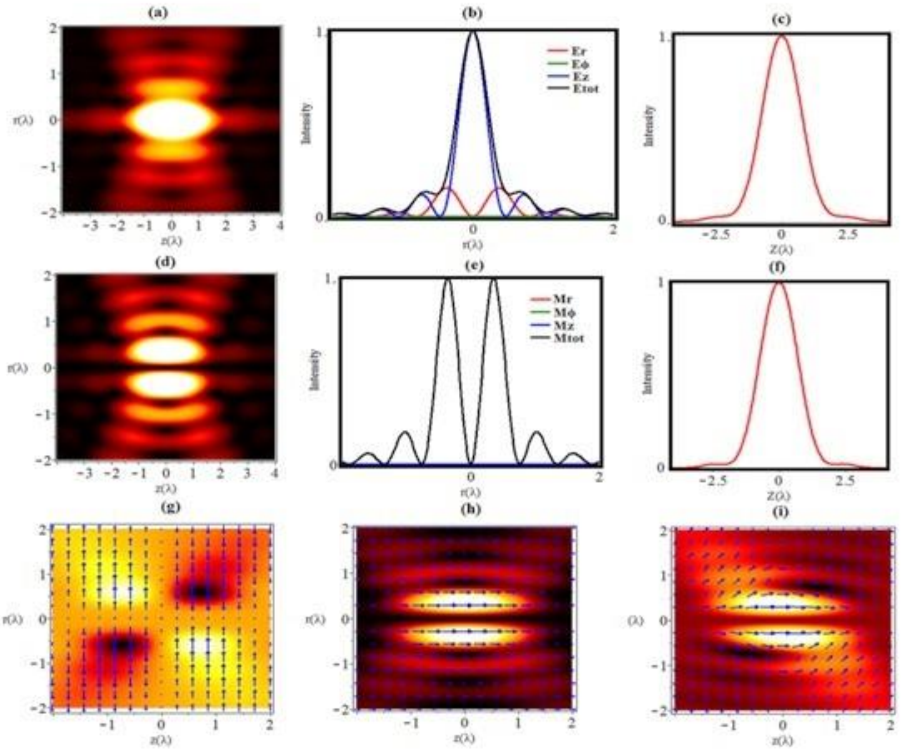

Figure 2 (a-f) Intensity distribution of the electric and magnetic field.(g-i) transverse, longitudinal and total components of the normalized Poynting vectors in the through-focus plane. For m=2 and C = 0

Figure 3 shows increasing order m of the multi Gaussian beam as 12 and by setting C=0,generated focal structure becomes an axially extended focal spot with dominating longitudinal component for the electric field distribution and an axially extended focal hole for the dominating (Mϕ) component magnetic field distribution as shown in figure (a) and (d) respectively. We noted that the FWHM of the electrical spot and magnetic hole is (0.36λ) and (4.1λ) respectively and the corresponding focal depth improved (0.9λ) and (4.2λ).figure (g-i) shows no energy flow along the axis and it's dominated by the longitudinal flow beside the axis. It is also noted that increasing the order of the focal depth .this is due to the fact.

Figure 3 shows increasing order m of the multi Gaussian beam as 12 and by setting C=0,generated focal structure becomes an axially extended focal spot with dominating longitudinal component for the electric field distribution and an axially extended focal hole for the dominating (Mϕ) component magnetic field distribution as shown in Figure (a) and (d) respectively. We noted that the FWHM of the electrical spot and magnetic hole is (0.36λ) and (4.1λ) respectively and the corresponding focal depth improved (0.9λ) and (4.2λ). Figure (g-i) shows no energy flow along the axis and its dominated by the longitudinal flow beside the axis. It is also noted that increasing the order of the focal depth .this is due to the fact.

Such flattop profile is useful in improved printing filling factor, improved uniformity and quality in materials processing, particle acceleration and microlithography [51-53]. The energy flow distribution of transverse and longitudinal component almost resemble the previous case however transverse energy flow along the axis is observed in the transverse component as shown in Figure (g). Figure (i) show that the total energy flow is null along the axis and it is found to be spiraling in the transverse direction from the focus.

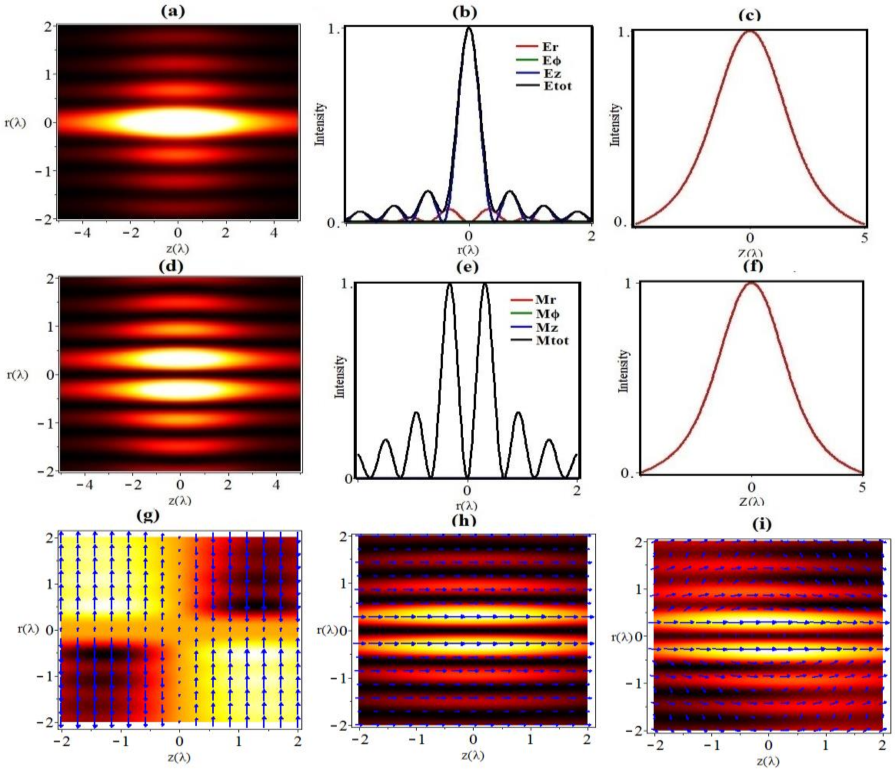

Figure.3. (a-f) Intensity distribution of the electric and magnetic field.(g-i) transverse, longitudinal and total components of the normalized Poynting vectors in the through-focus plane. For m=12 and C = 0.

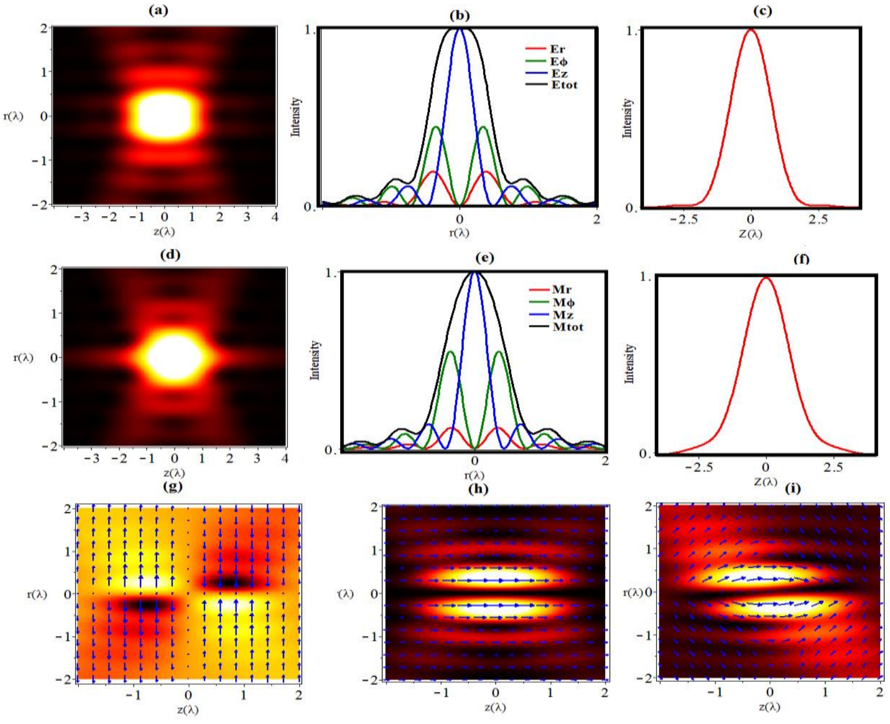

Figure 4 (a-f) Intensity distribution of the electric and magnetic field (g-i) transverse, longitudinal and total components of the normalized Poynting vectors in the through-focus plane.

For m=2 and C = 0.41.

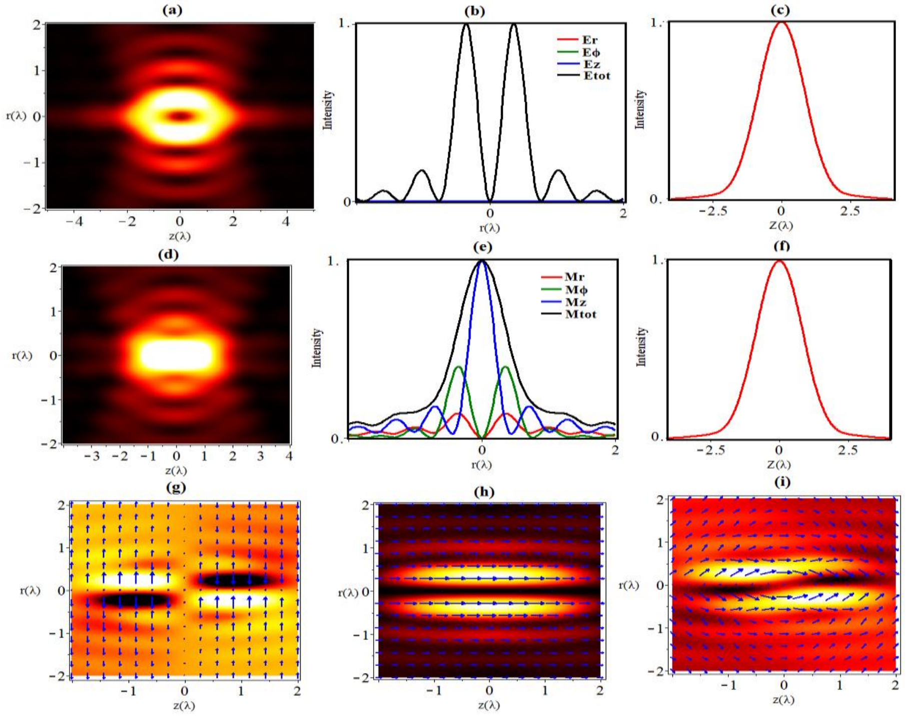

Figure 5 (a-f) Intensity distribution of the electric and magnetic field (g-i) transverse, longitudinal and total components of the normalized Poynting vectors in the through-focus plane. For m=2 and C = 1.0.

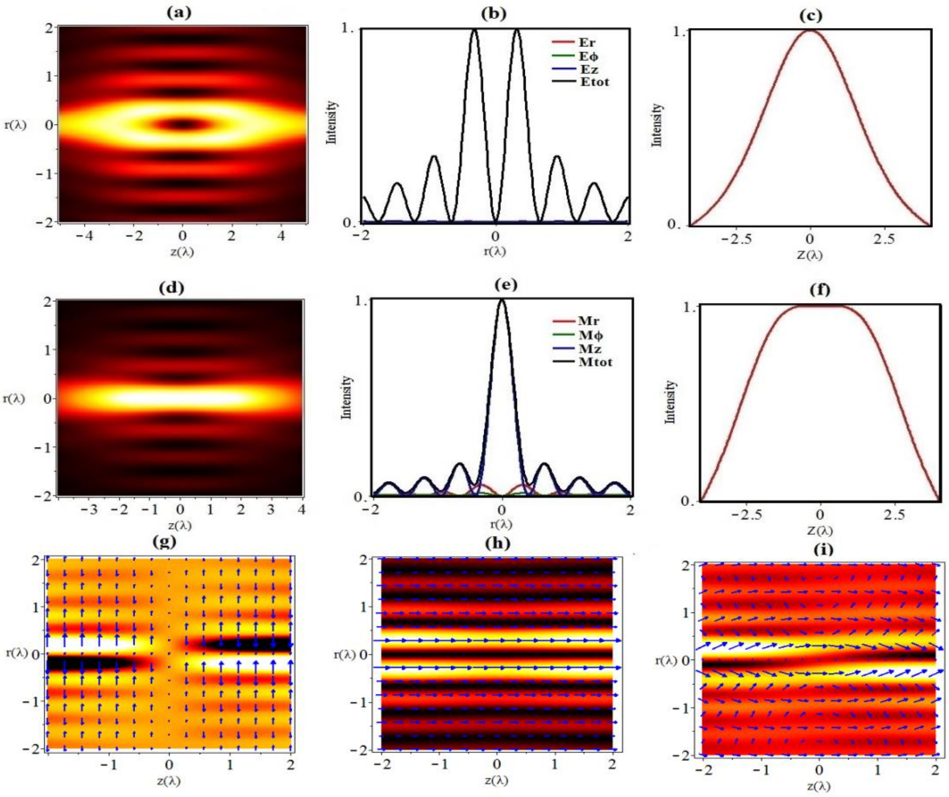

Figure.6.(a-f) Intensity distribution of the electric and magnetic field. (g-i) transverse, longitudinal and total components of the normalized Poynting vectors in the through-focus plane. For m=12 and C = 1.0.

Figure 5(a) shows same as Figure (2) but for spirality C=1.0. It is noted from the figure (a and d) increasing the spirality C as 1.0 generated an uniform intense optical bubble and an axially extended spot for the electric and magnetic field distribution with FWHM of 0.95λ.and DOF as 1.6λ respectively. It is noted from figure (b) and (e) that the total electric and magnetic field is dominated by the (Eϕ and Mz) components. Such cages have attracted significant attention in recent years because of the many actual and potential applications they have, such as for imaging [1,2], optical trapping [3,4], and optical cloaking [5]. It is observed from Figure (g-i) through the energy flow pattern of the transverse and longitudinal component resemble the previous case the total energy flow shows energy flow along the axis and it is spiraling in the transverses axis from the focus.

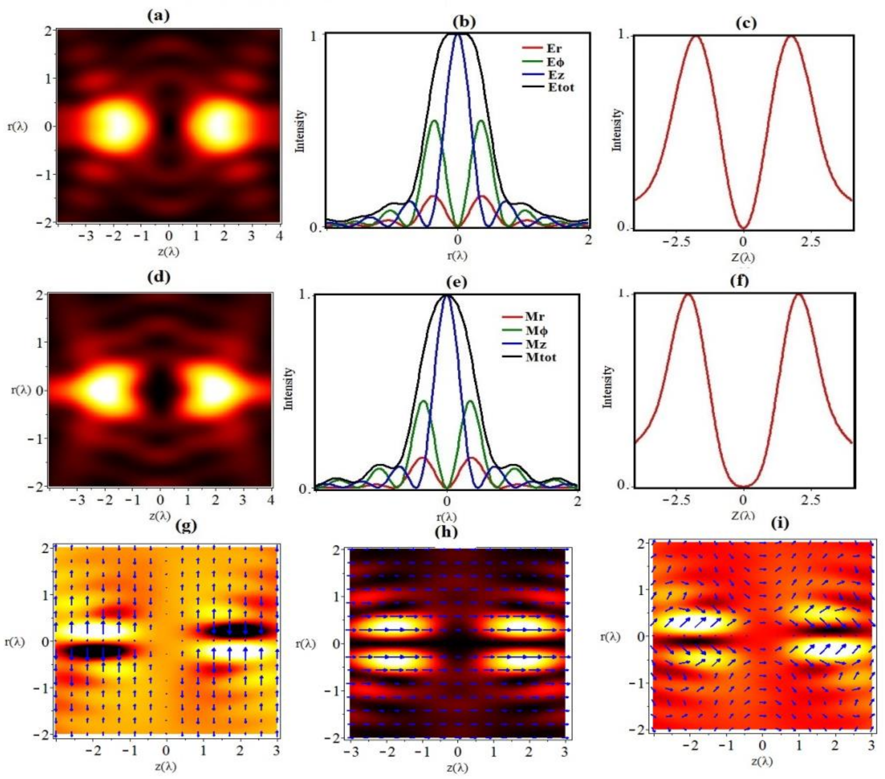

Figure 7(a-f) Intensity distribution of the electric and magnetic field. (g-i) transverse, longitudinal and total components of the normalized Poynting vectors in the through-focus plane. For m=2 and C = 2.78.

Figure 6 shows that by carefully setting C as 1.9, one can generate uniform intense optical bubble and a sharp magnetic spot with axial flattop profile for the electric and magnetic field distribution. Such a focal pattern has attractive application as mentioned previously. The magnetic spot with dominating longitudinal component is useful for application such as ultrahigh density all-optical magnetic recording and fabricating magnetic lattices for spin wave operation and atomic trapping with flexibility. Figure 6 (g-i) through the radial and longitudinal energy flow pattern resemble for the previous cases, however transverse energy flow is found at the focus and the energy flow spirals above and below the focus.

It is noted from the Figure 7 increasing the C as 2.78 spiral parameter the electric and magnetic field distribution as obtained is an axially splitted spots each having FWHM of 0.8λ and 2.8λ with DOF as (0.9λ) and (2.1λ).We noted that the electric field distribution is an flattop profile in the radial axis with dominating (Ez) component such a axially splitted focal spots are usable for high-density optical data storage, particle acceleration, biomedical imaging and in optical trapping [54-56]. Figure 7 (g) and (h) also shows that the transverse and longitudinal component of energy flow is also axially splitted. The total energy flow pattern show in figure (i) shows energy flow for the first spot is diverging whereas it is converging for the second spot along the radial axis from the focus. Such an energy flow pattern is usable for transporting particles from the first spot to second one. However, Figure (8) shows that setting m=12 and C=3.4, the DOF of the splitted spots extend to 4.1λ with FWHM of 0.35λ. It is also noted that the splitted magnetic spots obtained is irregular and dominated (Eφ) and (Ez) component and scene bumpy structure is observed. The energy flow pattern shown Figure 8(g-i) shows the converging and diverging transverse flow before and after flow with spiraling flow at the focus. Further, the directions of the transverse energy flows are reversed between these two regions, which are directed inwardly and outwardly along the radial direction, respectively. Overall, the proposed method may be help in applications like magnetic recording, magnetic resonance microscopy, and optical micromanipulation.

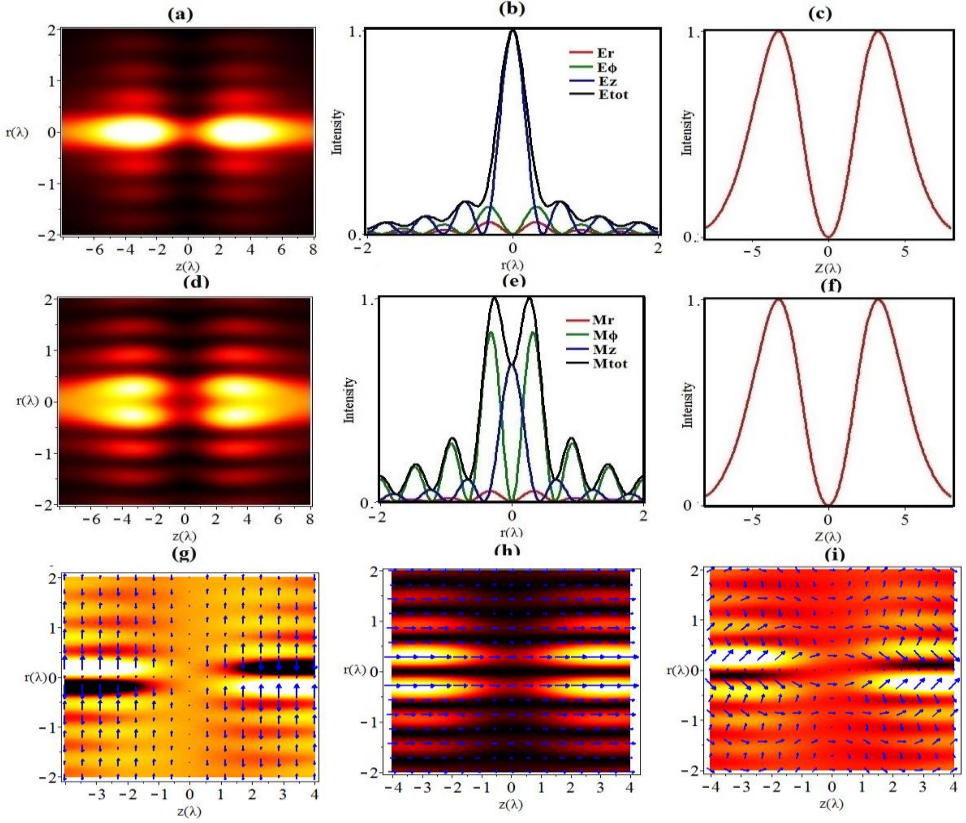

Figure 8(a-f) Intensity distribution of the electric and magnetic field. (g-i) transverse, longitudinal and total components of the normalized Poynting vectors in the through-focus plane, For m=12 and C = 3.4.

4. CONCLUSION

The tight focusing properties of spirally polarized annular multi Gaussian beam by High NA lens are investigated theoretically by vector diffraction theory. Results show that the optical intensity in focal region of spirally polarized annular multi Gaussian beam can be altered considerably by the beam order and spiral parameter. Spiral parameter can induce focal pattern change in axial direction remarkably and many novel focal patterns including optical bubbles, focal hole and focal spots of long focal depth and axially separated focal spots are evolved. We expect such tunable focal patterns are useful for optical manipulation of micro particles.

REFERENCES

[1] Zhan, Q., 2009. Cylindrical vector beams: from mathematical concepts to applications, Adv. Opt. Photon. 1, 1–57.

[2] Young, worth K.S, Brown, T.G., 2000. Focusing of high numerical aperture cylindrical vector beams, Opt. Express 7 77–87.

[3] Man, Z, Fu, S, Wei, G., 2017. Focus engineering based on analytical formulae fortightly focused polarized beams with arbitrary geometric

configurations of linear polarization, J. Opt. Soc. Am. A 34, 1384–1391.

[4] Zhan,. Q, Leger, J.R. 2002. Focus shaping using cylindrical vector beams, Opt. Express 10, 324–331.

[5] Qiwen Zhan., 2006. Properties of circularly polarized vortex beams, Opt. Lett. 31, 867–869.

[6] Kozawa, Y, Sato, S., 2007. Sharper focal spot formed by higher-order radially polarized laser beams, J. Opt. Soc. Am. A 24,1793–1798.

[7] Chen, G.Y., Song, F, Wa, H.T, 2013. Sharper focal spot generated by 4πtight focusing of higher-order Laguerre-Gaussian radially polarized beam, Opt. Lett. 38, 3937–3940.

[8] Hao, X, Kuang, C, Wang, T, Liu X., 2010. Phase encoding for sharper focus of the azimuthally polarized beam, Opt. Lett. 35 3928–3930.

[9] Man, Z , Bai, Z, Zhang, S, Li, J, Li, X, Ge X, Zhang, Y, Fu, S., 2018. Focusing properties of arbitrary optical fields combing spiral phase and cylindrically symmetric state of polarization, J. Opt. Soc. Am. A 35, 1014–1020.

[10] Guo H, Dong X, Weng X, Sui G, Yang N, Zhuang S., 2011. Multifocus with small size, uniform intensity, and nearly circular symmetry, Opt. Lett. 36, 2200–2202.

[11] Huang K, Shi P, Cao G.W., Li K, Zhang X.B., Li Y.P., 2011. Vector-vortex Bessel-Gauss beams and their tightly focusing properties, Opt. Lett. 36, 888–890.

[12] Cai M, Tu C, Zhang H, Qian S, Lou K, Li Y, Wang, H.T., 2013. Sub wavelength multiple focal spots produced by tight focusing the patterned vector optical field, Opt. Express 21, 31469–31482.

[13] Li, P, Guo, X, Qi S, Han, L, Zhang Y, Liu S, Li, Y, Zhao, J., 2018. Creation of independently controllable multiple focal spots from segmented Pancharatnam-Berry phases, Sci. Rep. 8, 9831.

[14] Wang, H, Shi, L, Lukyanchuk B, C. Sheppard, Chong C.T., 2008. Creation of a needle of longitudinally polarized light in vacuum using binary optics, Nat. Photon. 2, 501–505.

[15] Yuan, G.H., Wei, S.B, Yuan, X.C., 2011. Non diffracting transversally polarized beam, Opt.Lett. 36, 3479–3481.

[16] Dehez H, April A, Piché M., 2012. Needles of longitudinally polarized light: guidelines for minimum spot size and tunable axial extent, Opt. Express 20 14891–14905.

[17] Man, Z, Min, C, Du, L, Zhang, Y, Zhu, S, Yuan, X, 2016. Sub-wavelength sized transversely polarized optical needle with exceptionally suppressed side-lobes, Opt. Express 26, 874–882.

[18] Wang X, Zhu B, Dong Y, Wang S, Zhu Z, Bo F, Li X, 2017. Generation of equilateral-polygon-like flat-top focus by tightly focusing radially polarized beams superposed with off-axis vortex arrays, Opt. Express 25, 26844–26852.

[19] Zhao, Y, Zhan, Q, Zhang, Z, Li, Y.P, 2005. Creation of a three-dimensional optical chain for controllable particle delivery, Opt. Lett. 30, 848–850.

[20] Wang, J, Chen,W, Zhan, Q., 2012 Creation of uniform three-dimensional optical chain through tight focusing of space-variant polarized beams, J. Opt. 14, 055004.

[21] Lin, H, Jia, B, Gu, M., 2011.Dynamic generation of Debye diffraction-limited multifocal arrays for direct laser printing nanofabrication, Opt. Lett. 36, 406–408.

[22] Lin, H, Gu, M., 2013. Creation of diffraction-limited non-Airy multifocal arrays using s spatially shifted vortex beam, Appl. Phys. Lett. 102, 084103.

[23] Zhu L, Yu J, Zhang D, Sun M, Chen J, 2014 Multifocal spot array generated by fractional Talbot effect phase-only modulation, Opt. Express 22, 9798–9808.

[24] Zeng, T, Chang, C, Chen, Z, Wang H.T, Ding J, 2018. Three-dimensional vectorial multifocal arrays created by pseudo-period encoding, J. Opt. 20, 065605.

[25] Guan, J, Liu, N, Chen, C, Huang, X, Tan J, Lin, J, Jin P, 2018. Non-iterative dartboard phasefilter for achieving multifocal arrays by cylindrical vector beams, Opt. Express 26, 24075–24088.

[26] Tian, B, Pu, J, 2014. Tight focusing of a double-ring-shaped azimuthally polarized beam, Opt. Lett. 36, 2014–2016.

[27] Shu, J, Chen, Z, Pu, J, Liu, Y., 2014. Tight focusing of a double-ring-shaped, azimuthally polarized beam through a

dielectric interface, J. Opt. Soc. Am. A 31, 1180–1185.

[28] Wei L, Urbach H.P, 2016. Shaping the focal field of radially / azimuthally polarized phase vortex with Zernike polynomials, J. Opt. 18, 065608.

[29] Weng, X, Du, L, Shi, P, Yuan, X., 2017. Creating adjustable uniform optical cages through polarization shaping in a low NA optical system, Appl. Opt. 56, 1046–1051.

[30] Weng, X, Du, L, Shi, P, Yuan, X, 2017. Tunable optical cage array generated by Dammann vector beam, Opt. Express 25, 9039–9048.

[31] Man, Z, Bai, Z, Li, J, Zhang, S, Li, X, Zhang, Y, Ge X, Fu S,2018. Optical cage generated by azimuthal- and radial-variant vector beams, Appl. Opt. 57, 3592–3597.

[32] Bokor, N, Davidson, N, Towards., 2004. spherical spot distribution with 4πfocusing of radially polarized light, Opt. Lett. 29, 1968–1970.

[33] Chen, W, Zhan, Q, 2009. Creating a spherical focal spot with spatially modulated radial polarization in 4Pi microscopy, Opt. Lett. 34, 2444–2446.

[34] Lin H, Jia B, Gu M, 2011 Generation of an axially super-resolved quasi-spherical focal spot using an amplitude-modulated radially polarized beam, Opt. Lett. 36, 2471–2473.

[35] Yan S, Yao B, Rupp R, 2011. Shifting the spherical spot of a 4Pi focusing system, Opt. Express 19, 673–678.

[36] Zhang, Y, Wang, J, Shen, J, Man, Z, Shi, W, Min, C, Yuan, G, Zhu, S, Urbach, H.P, X. Yuan, 2014. Plasmonic hybridization induced trapping and manipulation of a sing Au nanowire on a metallic surface, Nano Lett. 14, 6430–6436.

[37] Min, C, Shen, Z, Shen, J, Zhang, Y, Fang, H, Yuan G, Du L, Zhu S, Lei T, Yuan X, 2013. Focused plasmonic trapping of metallic particles, Nat. Commun. 4, 2891.

[38] Kozawa, Y, Matsunaga, D, Sato S, 2018. Super resolution imaging via superscillation focusing of a radially polarized beam, Optica 5, 86–92.

[39] Zhang Y Bai J., 2009. Improving the recording ability of a near-field optical storage system by higher-order radially polarized beams, Opt. Express 17, 3698–3706.

[40] Xu J, Yang Z.J, Li J.X, Zang W.P, 2017. Electron acceleration by a tightly focused cylindrical vector Gaussian beam, Laser Phys. Lett. 14, 025301.

[41] Hao, B., Leger, J., 2008. Numerical aperture invariant focus shaping using spirally polarized beams. Opt. Commun. 281(8), 1924–8.

[42] Ramírez-Sánchez V, Piquero G, Santarsiero M, 2009. Generation and characterization of spirally polarized fields. J. Opt. A Pure Appl. Opt. **11**, 085708-1–085708-6.

[43] Pu, J, Zhang, Z, 2010., Tight focusing of spirally polarized vortex beams. Opt. Laser Technol.**42**, 186–191.

[44] Gao, X, Zhan Q, Li J, Wang J, Zhuang S, 2011. Spirally polarized axisymmetric Bessel-modulated Gaussian beam. Optik 122, (2011)524–528.

[45] Suresh, P,, Mariyal, C, Sarswathi, R.C., Rajesh, K.B., Pillai T.V.S., Jaroszewicz Z, 2014. Tightly focusing of spirally polarized Quadratic Bessel Gaussian beam through a dielectric interface . Optik 125 , 1264– 1266.

[46] Senthilkumar, M., Rajesh, K.B., Udhayakumar, M, Jaroszewicz, Z, Mahadevan, G., 2019. Focusing properties of spirally polarized sinh Gaussian beam Optics and Laser Technology 111, 623–628

[47] Angelsky O.V, Gorsky M.P, Maksimyak P.P, Maksimyak A.P, Hanson S.G., and. Yu C,Zenkova., 2011. Investigation of optical currents in coherent and partially coherent vector fields, Opt. Express 19(2), 660–672.

[48] Fries,e M.E.J, Enger, J, Rubinsztein-Dunlop, H, and Heckenberg N.R., 1996. Optical angular-momentum transfer to trapped absorbing particles, Phys. Rev. A 54(2), 1593–1596.

[49] Richards, B, Wolf, E., 1959. Electromagnetic diffraction in optical systems II. Structure of the image field in a planatic system, Proc. R. Soc. London Ser. A 253, 358–379.

All © 2022 are reserved by International Journal of Advanced Science and Engineering. This Journal is licensed under a Creative Commons Attribution-Non Commercial-ShareAlike 3.0 Unported License.